Effect of pH, NaCl, CaCl₂ and Temperature on Self-Assembly of β-Lactoglobulin into Nanofibrils: A Central Composite Design Study

S. M. Loveday,*,[†] X. L. Wang,[†] M. A. Rao,[‡] S. G. Anema,[§] and H. Singh[†]

[†]Riddet Institute, Massey University, Private Bag 11 222, Palmerston North, New Zealand
[‡]Department of Food Science, Cornell University, Geneva, New York 14456, United States
[§]Fonterra Research Centre, Dairy Farm Road, Private Bag 11029, Palmerston North, New Zealand

Ⓢ Supporting Information

ABSTRACT: The ability of certain globular proteins to self-assemble into amyloid-like fibrils *in vitro* opens opportunities for the development of new biomaterials with unique functional properties, like highly efficient gelation and viscosity enhancement. This work explored the individual and interacting effects of pH (1 to 3), NaCl (0−100 mM), CaCl₂ (0−80 mM) and heating temperature (80 to 120 °C) on the kinetics of β-lactoglobulin self-assembly and the morphology of resulting nanofibrils. Statistically significant ($p < 0.05$) interactions included CaCl₂*temperature, NaCl*pH, CaCl₂*pH, temperature*pH and NaCl*CaCl₂. Particularly notable was the very rapid self-assembly at pH 3 and the highly nonlinear effect of pH on self-assembly kinetics. Nanofibril morphologies ranged from long and semiflexible or curled and twisted to short and irregular. There did not seem to be a link between the kinetics of fibril formation and the morphology of fibrils, except at pH 3, where self-assembly was very rapid and fibrils were short and irregular, suggesting haphazard, uncontrolled self-assembly.

KEYWORDS: protein, beta-lactoglobulin, whey protein, self-assembly, nanofibril, amyloid, acid hydrolysis, heat, thioflavin T, transmission electron microscopy, central composite design

■ INTRODUCTION

Many proteins can self-assemble *in vitro* into fibrils consisting of stacked β-sheets, which are structurally similar to amyloid fibrils seen *in vivo* in association with certain neurological disorders. Several globular food proteins such as ovalbumin and lysozyme from eggs, glycinin from soy and bovine serum albumin and β-lactoglobulin from milk form "amyloid-like" fibrils *in vitro* under certain denaturing conditions. Fibrils form in a matter of days at 20−37 °C in concentrated guanidinium[1] or organic solvents,[2] or in a few hours at elevated temperature, low pH and low ionic strength.[3]

Amyloid-like protein fibrils typically form viscoelastic gels at low protein concentration, and for that reason they may have applications as tissue scaffolds[4] or texture-enhancing food ingredients. Other applications such as enzyme immobilization[5] and encapsulation of bioactives[6] have also been explored.

Both the rate of self-assembly and the morphology of amyloid-like β-lactoglobulin fibrils formed *in vitro* depend on environmental factors, and they are often linked. For example, the rate of self-assembly can be enhanced by shearing[7] but the fibril length distribution is shifted to shorter lengths and becomes more polydisperse.[8] Similarly, self-assembly is accelerated by adding salts, but with ≥60 mM NaCl or ≥33 mM CaCl₂, fibrils change from being long and semiflexible to short and tightly curled.[3] Functional properties also change; for example, fibrils made at 100 °C and pH 2 give more viscous dispersions than those made at 80 °C.[9]

A number of efforts have been made to quantify the effects of individual environmental variables on protein self-assembly into amyloid-like fibrils. For example, Pearce, Mackintosh, and Gerrard[10] showed how NaCl, protein concentration and heating temperature affected the self-assembly of ovalbumin, egg white and bovine serum albumin. Mudgal, Daubert, and Foegeding[11] measured the properties of β-lactoglobulin fibrils made at different pH and protein concentrations. Kroes-Nijboer, Venema, Bouman, and van der Linden[12] reported the effect of protein concentration and heating temperature on fibril yield and critical aggregation concentration.

However we have found no previous research using statistically rigorous experimental designs to look at interacting effects of environmental factors on protein self-assembly into amyloid-like fibrils. Here we set out to quantify the interactions between heating temperature, NaCl concentration, CaCl₂ concentration and pH, all of whose individual effects are understood from our previous work.[3,9]

■ MATERIALS AND METHODS

Chemicals. Thioflavin T powder, HCl and β-lactoglobulin (90% pure), containing a mixture of genetic variants A and B, were purchased from Sigma-Aldrich (St. Louis, MO). NaCl and CaCl₂ were AnalaR grade from BDH (Poole, England). Milli-Q water was used throughout the study.

Preparation of β-Lactoglobulin Solutions. Milli-Q water was adjusted to the required pH (±0.05) with 6 M HCl, and β-lactoglobulin was added to make a 1.2% w/v dispersion. Although proteins have some buffering capacity, the pH did not shift when β-lactoglobulin was stirred

Table 1. Experimental Design, Fitting Diagnostics and Kinetic Parameters Derived from ThT Fluorescence Data[a]

point type	run no.	NaCl (mM)	CaCl$_2$ (mM)	temp (°C)	pH	adjusted R^2	$S_{y\|x}$	$t_{\text{ThT max}}$ (h)	$(\mathrm{d}f/\mathrm{d}t)_{max}$ (FU·h^{-1})	ThT$_{max}$ (FU)
center	1	50	40	100	2.0	0.95	10.1	4.4	54.5	131.9
	2	25	20	90	1.5	0.96	16.9	6.2	69.3	205.3
	3	75	20	90	1.5	0.93	20.6	5.4	73.6	254.7
	4	25	60	90	1.5	0.94	17.3	4.0	186.0	247.7
	5	75	60	90	1.5	0.97	14.5	2.1	**399.3**[3]	**319.8**[3]
	6	25	20	110	1.5	0.82	13.7	**1.6**[2]	177.5	132.5
	7	75	20	110	1.5	0.87	25.2	**1.7**[3]	**392.4**[4]	274.4
	8	25	60	110	1.5	0.87	25.7	2.3	311.8	260.1
factorial points	9	75	60	110	1.5	0.82	40.0	**1.8**[4]	**474.8**[2]	**369.4**[2]
	10	25	20	90	2.5	0.98[b]	7.7	15.9	15.7	168.3
	11	75	20	90	2.5	0.95	18.2	6.5	63.0	272.6
	12	25	60	90	2.5	0.98	11.7	6.4	88.2	256.8
	13	75	60	90	2.5	0.90	27.9	2.5	362.3	**297.5**[4]
	14	25	20	110	2.5	0.91	12.8	6.1	14.1	121.8
	15	75	20	110	2.5	0.91	12.8	3.1	127.4	146.6
	16	25	60	110	2.5	0.82	26.4	3.1	122.9	207.5
	17	75	60	110	2.5	0.93	20.9	2.4	321.9	**291.7**[5]
center	18	50	40	100	2.0	0.94	10.7	5.0	34.4	103.1
	19	0	40	100	2.0	0.91	23.7	4.6	89.3	234.6
	20	100	40	100	2.0	0.92	19.5	2.9	251.8	263.0
	21	50	0	100	2.0	0.96[c]	13.7	18.0	29.7	207.1
	22	50	80	100	2.0	0.97	10.8	2.7	231.0	211.6
star points	23	50	40	80	2.0	0.98	12.7	14.1	30.2	226.4
	24	50	40	120	2.0	0.95	16.2	**1.3**[1]	**379.9**[5]	221.1
	25	50	40	100	1.0	0.96	15.5	2.1	328.1	255.5
	26	50	40	100	3.0	0.96	35.7	**2.0**[5]	**868.6**[1]	**662.8**[1]
center	27	50	40	100	2.0	0.85	18.7	4.7	63.8	117.3

[a] The parameters t_{ThTmax} and $(\mathrm{d}f/\mathrm{d}t)_{max}$ were derived from 6th-order polynomial fitting of ThT fluorescence data (see Supporting Information for analytical derivations), while ThT$_{max}$ is the experimentally measured maximum ThT fluorescence (mean of three measurements). Bold typeface and superscript numbers indicate the top five entries in each results column, where "top" is the lowest for t_{ThTmax} and the highest for other parameters. [b] Run 10 data were fitted with a 5th order polynomial function. [c] Run 21 data were fitted with a 3rd order polynomial function.

in, probably because of the low protein concentration. The solution was stirred overnight at 4 °C, then centrifuged at 22600g for 30 min (Himac CR22G II super speed centrifuge, Hitachi Koki Co., Japan) and filtered (0.2 μm syringe filter, Millex-GS, Millipore, Billerica, MA).

Residual salts were removed by ultrafiltration using a centrifugal filter (10 kDa cutoff, Amicon Ultra-15, Millipore) by centrifuging at 3000g for 15 min. Filters were rinsed with pH 2 water prior to use. The retentate was topped up to the original volume with buffer, and filtering was repeated two more times. After three filtration steps, the conductivity of the protein solution was close to that of pH 2 water.

Protein concentration in the desalted β-lactoglobulin solution was determined by absorption at 278 nm (Ultrospec 2000 UV spectrophotometer, Pharmacia Biotech, Cambridge, U.K.), using a β-lactoglobulin standard curve and assuming 90% purity, as stated by the supplier. A small proportion of protein was lost during centrifuging and filtering, and an initial concentration of 1.2% w/v gave a final concentration close to 1% w/v. Solutions of β-lactoglobulin were stored at 4 °C and used within two days of preparation.

NaCl and CaCl$_2$ concentrations were adjusted using 1 M solutions, and final volumes were adjusted to the same level with water to avoid dilution effects.

Heating of β-Lactoglobulin Solutions. Aliquots of β-lactoglobulin solution (2 mL) in screw-capped glass tubes (16 mm diameter Kimax glass, Schott, Elmsford, NY) were heated in a dry block heater (Techne DB-3D, Bibby Scientific Ltd., Staffordshire, U.K.). Following

the requisite heating time, a tube was cooled in ice water for 5−10 min. To check for water loss during heating, tubes containing only water were heated for 4 h at 80−120 °C and weighed every hour.

Thioflavin T (ThT) Fluorescence Assay. A stock solution of 3.0 mM ThT in phosphate-NaCl buffer (10 mM phosphate and 150 mM NaCl, pH 7.0) was filtered through a 0.2 μm syringe filter (Millex-GS, Millipore). The stock solution was stored at 4 °C in a brown glass bottle covered with aluminum foil. Working solution was prepared by diluting the stock solution 50-fold in phosphate-NaCl buffer (final ThT concentration 60 μM).

In the assay, 48 μL of sample was added to 4 mL of working solution; the mixture was vortexed briefly and held at room temperature for 1 min before measuring fluorescence (RF-1501 spectrofluorimeter, Shimadzu, Kyoto, Japan). Excitation and emission wavelengths were 440 and 482 nm, respectively. The fluorescence of unheated protein solution was subtracted from all measurements. ThT fluorescence readings were corrected for water loss using the measured rates of mass loss from heated tubes of water.

Negative Stain Transmission Electron Microscopy (TEM). The ultrafiltration method of Bolder, Vasbinder, Sagis, and van der Linden[13] was used to purify fibrils and reduce the background in TEM images. 100 μL of heated protein solution was added to 2 mL of pH 2 water in a centrifuge filter (100 kDa cutoff, Amicon Ultra-4, Millipore), which had been previously washed with 2 mL of pH 2 water. The filter was centrifuged at 3000g for 15 min, the filtrate was discarded and 2 mL

of pH 2 water was added to the retentate. The sample was centrifuged again, retentate topped up with 2 mL of pH 2 water, centrifuged a third time, then 1 mL of pH 2 water was added to the retentate, mixed by inversion and transferred to a 1.5 mL plastic tube (Eppendorf, Hamburg, Germany). The final dilution of heated protein was approximately 10-fold.

A copper TEM grid coated with Formvar was placed on a droplet of sample for 5 min. The grid was removed, touched against filter paper to soak away excess sample and then placed on a drop of 2% uranyl acetate in water for 5 min. Excess stain was soaked away with filter paper. The negatively stained grid was examined with a Philips CM10 electron microscope (Eindhoven, The Netherlands).

Image contrast was improved by contrast-stretching with Adobe Photoshop Elements 2.0 (Adobe Systems Inc., San Jose, CA).

Fluorescence Curve Fitting. ThT fluorescence data were fitted with polynomial curves using SigmaPlot 10.0 (Systat software, Chicago, IL), which was also used for plotting graphs. Kinetic parameters are defined as follows:

t_{ThTmax}: the time at which the fitted function reaches its first local maximum or plateau

$(df/dt)_{max}$: the maximum rate of increase of the fitting function between $t = 0$ and $t = t_{ThTmax}$

ThT_{max}: the global maximum measured value of ThT fluorescence

The analytical derivations of t_{ThTmax} and $(df/dt)_{max}$ are given in the Supporting Information.

Statistical Design and Analysis. Minitab 15 (Minitab Inc., State College, PA) was used for experimental design and for analysis of results by response surface and factorial regression. The design was a four-factor central composite circumscribed design with triplicate center point runs.[14] Due to the number of factors, star points were twice as far from center point as were factorial points, i.e. $\alpha = 2$. Factor settings are shown in Table 1.

■ RESULTS

ThT Fluorescence Fitting and Kinetic Parameters. ThT fluorescence data were fitted with polynomial functions as a means of interpolating data in a way that allowed unbiased determination of kinetic parameters. The model used in earlier work[3] was not suitable because lag phases in the present work were often very short or absent. Polynomial equations were used because they were flexible enough to fit several different time-course shapes, they were simple to fit and they were analytically convenient. No mechanistic significance was attributed to the function coefficients, and only the portion of the curve up to the first local maximum or inflection point was used for deriving kinetic parameters. Fitting the data in this way provided continuously variable values of t_{ThTmax}, which could be statistically analyzed in a way that the discretely varying time point values could not.

The sixth-order polynomial function fitted data well in most cases, indicated by adjusted R^2 values close to 1 and relatively low estimated standard error of the regression, $S_{y|x}$ (Table 1). Selected data series are shown in Figure 1. The adjusted R^2 was only 0.82 for runs 6, 9 and 16, because the fluorescence did not vary smoothly with time; see for example run 9 data in Figure 1.

Figure 1 shows that there was some fluctuation in fluorescence after the initial maximum in ThT fluorescence had been reached, particularly for run 26. If fibril volume fraction can be assumed to remain constant once the maximum is reached, this fluctuation suggests that there was some variation in fibril volume fraction between assay aliquots and some spatial heterogeneity in samples. We observed a similar phenomenon in earlier work,[3]
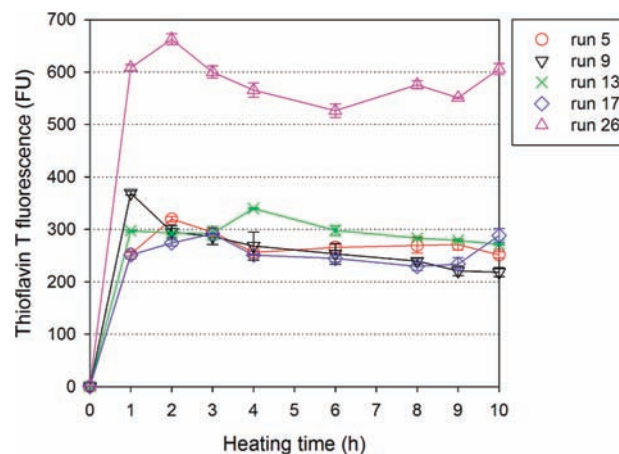

Figure 1. Thioflavin T fluorescence data for selected runs which showed rapid increase in ThT fluorescence and high maximum ThT fluorescence. Vertical bars are standard errors from triplicate assays.

and attributed this to local gelation, as indicated by small gel particles visible in some samples.

The function fitted the data of run 21 well, but the fit curve was not a reasonable shape, since it had a peak at 14 h followed by a deep, narrow trough at 22 h. Data from this run were instead fitted with a cubic function (adjusted $R^2 = 0.96$), and the inflection point at 18 h was taken as t_{ThTmax}. Similarly, the sixth-order fit of data from run 10 had a large, sharp peak at 22 h, which was inconsistent with the expected plateau in fluorescence. A fifth-order polynomial function was a more sensible shape, and was a very accurate fit (adjusted $R^2 = 0.98$).

Statistical Analysis of ThT Fluorescence. The values of t_{ThTmax}, $(df/dt)_{max}$ and ThT_{max} for each experimental run are listed in Table 1, with the best-performing runs (lowest t_{ThTmax}, highest $(df/dt)_{max}$ and ThT_{max}) highlighted with bold type and superscript rankings. Both t_{ThTmax} and $(df/dt)_{max}$ are measures of the initial rate of increase in ThT fluorescence, and they were strongly correlated ($r = -0.85$, $p < 0.001$) when obvious outliers (runs 10, 21, 23 and 26) were removed. There was also a reasonably strong correlation ($r = 0.70$, $p < 0.001$) between $(df/dt)_{max}$ and ThT_{max}, once run 26 was removed as an outlier. This is not surprising, because $(df/dt)_{max}$ is derived from an equation designed to fit the peak in ThT fluorescence. Plotting t_{ThTmax} vs ThT_{max} showed several obvious outliers (runs 10, 21, 23 and 26), but when these were removed there was no correlation ($r = -0.34$, $p = 0.118$). This means that the time to reach a peak in ThT fluorescence was not related to the height of the peak, i.e. maximum yield of fibrils. In other words, conditions under which ThT fluorescence increases most rapidly may not be those in which the yield of fibrils is highest.

Values for t_{ThTmax}, $(df/dt)_{max}$ and ThT_{max} were analyzed with two statistical techniques: response surface regression of the whole data set and factorial regression of only the factorial points and center points. The regression coefficients are shown in Table 2 (response surface analysis) and Table 3 (factorial analysis), and their statistical significance is indicated with shading: dark gray means $p > 0.05$, light gray means $0.01 < p \leq 0.05$ and no shading means $p \leq 0.01$. The factorial regression was necessary because runs 21, 23, and 26 proved to be extreme outliers, and they increased the overall variability of the data set such that response surface regressions were not very successful. The adjusted R^2

8469

dx.doi.org/10.1021/jf201870z |*J. Agric. Food Chem.* 2011, 59, 8467–8474

Table 2. Coefficients from the Response Surface Regressions of ThT Fluorescence Kinetic Parameters[a]

RESPONSE SURFACE ANALYSIS				
Effect type	Effect	$t_{ThT\ max}$	$(df/dt)_{max}$	ThT_{max}
1-FACTOR	NaCl	-2.0	129.5	57.0
	CaCl$_2$	-4.4	144.7	56.9
	temperature	-4.4	115.4	-19.1
	pH	1.7	9.3	42.8
2-WAY	NaCl*CaCl$_2$	1.6	117.4	-3.5
	NaCl*temperature	3.0	37.8	23.4
	NaCl*pH	-3.5	9.6	-29.7
	CaCl$_2$*temperature	4.0	-73.5	58.1
	CaCl$_2$*pH	-3.1	4.0	3.5
	temperature*pH	-1.6	-142.8	-59.1
QUADRATIC	NaCl*NaCl	-2.0	68.9	100.6
	CaCl$_2$*CaCl$_2$	4.6	28.8	61.2
	temperature*temperature	2.0	103.5	75.6
	pH*pH	-3.6	496.7	311.0
adjusted R^2 for the regression		0.64	0.40	0.56

[a] Regressions were done using coded units, so coefficients within a column are directly comparable with one another, but cannot be compared across rows. Dark gray shading indicates that $p \geq 0.05$ for a given coefficient, light gray shading indicates that $0.01 \leq p < 0.05$ and no shading indicates that $p < 0.01$.

Table 3. Coefficients from the Factorial Regression of ThT Fluorescence Kinetic Parameters[a]

FACTORIAL ANALYSIS				
Effect type	Effect	$t_{ThT\ max}$	$(df/dt)_{max}$	ThT_{max}
1-FACTOR	NaCl	-1.3	76.8	39.2
	CaCl$_2$	-1.4	83.4	42.1
	temperature	-1.7	42.8	-13.7
	pH	1.3	-60.6	-18.8
2-WAY	NaCl*CaCl$_2$	0.4	29.4	-0.9
	NaCl*temperature	0.7	9.5	5.9
	NaCl*pH	-0.9	2.4	-7.4
	CaCl$_2$*temperature	1.0	-18.4	14.5
	CaCl$_2$*pH	-0.8	1.0	0.9
	temperature*pH	-0.4	-35.7	-14.8
3-WAY	NaCl*CaCl$_2$*temperature	-0.2	-25.1	4.3
	NaCl*CaCl$_2$*pH	0.6	9.7	0.4
	NaCl*temperature*pH	0.5	-10.6	-10.4
	CaCl$_2$*temperature*pH	0.2	9.8	0.2
4-WAY	NaCl*CaCl$_2$*temperature*pH	-0.2	7.5	11.2
adjusted R^2 for the regression		0.99	0.99	0.85

[a] Regressions were done using coded units, so coefficients within a column are directly comparable with one another, but cannot be compared across rows. Dark gray shading indicates that $p \geq 0.05$ for a given coefficient, light gray shading indicates that $0.01 \leq p < 0.05$ and no shading indicates that $p < 0.01$.

Table 4. Mean Values of ThT_{max} for a Range of Settings of Temperature and NaCl Concentration[a]

Temperature Effects					
temp (°C)	80	90	100	110	120
mean ThT_{max}	226.4	252.8 (17.1)	243.0 (56.1)	225.5 (31.2)	221.1
no. of runs	1	8	9	8	1
NaCl Concentration Effects					
NaCl (mM)	0	25	50	75	100
mean ThT_{max}	234.6	200.0 (19.3)	237.4 (56.1)	278.3 (22.6)	263.0
no. of runs	1	8	9	8	1

[a] Standard errors among runs are shown in parentheses, except where there was only one run at given temperature and NaCl settings.
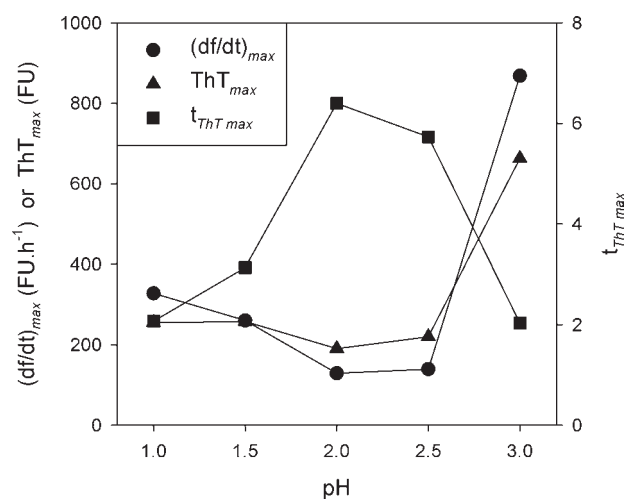

Figure 2. Effect of pH on $(df/dt)_{max}$, ThT_{max} and t_{ThTmax}. Each data point is the mean from all runs at that pH, i.e. 9 runs at pH 2.0, 8 runs at pH 1.5 and pH 2.5, and a single run at pH 1.0 and pH 3.0 (star points).

ThT_{max} mean values were not large. However pH had large nonlinear effects, as shown in Figure 2. Kinetic parameters were relatively constant at pH 2.0–2.5, but decreasing or increasing the pH caused $(df/dt)_{max}$ and ThT_{max} to increase while t_{ThTmax} decreased.

Both response surface and factorial regressions showed that CaCl$_2$ had a highly significant and moderately strong effect on ThT fluorescence, decreasing t_{ThTmax} and increasing $(df/dt)_{max}$ and ThT_{max}. In the factorial analysis (Table 3), CaCl$_2$ had significant and weak to moderate interactions with temperature for all three parameters. The CaCl$_2$*temperature effect on t_{ThTmax} is shown in Table 5. At 90 °C, increasing CaCl$_2$ from 20 mM to 60 mM had a large effect, whereas at 110 °C the effect was much smaller. The CaCl$_2$*temperature effect on $(df/dt)_{max}$ and ThT_{max} was significant but small (data not shown).

Both NaCl*pH and CaCl$_2$*pH had a significant and moderately strong effect on t_{ThTmax}, shown in Table 5. Increasing the amount of NaCl or CaCl$_2$ had a small effect at pH 1.5 and a large effect at pH 2.5. However these interactions had small and nonsignificant effects on $(df/dt)_{max}$ and ThT_{max}.

The temperature*pH effects on $(df/dt)_{max}$ and ThT_{max} were significant and moderately strong. Table 6 shows that increasing the temperature from 90 to 110 °C increased $(df/dt)_{max}$ more at pH 1.5 than at pH 2.5. The effect of this interaction on ThT_{max} is

values for factorial regressions, which did not include star points, were much higher than for response surface regressions, indicating a better fit.

In the response surface regression, 1-factor effects were significant for some variables and some kinetic parameters, but in the factorial analysis all individual variables had significant effects on all parameters. This probably reflects the effect of extreme outliers among the star points in the response surface analysis, as discussed above.

No 2-way interactions were significant in the response surface analysis, but some quadratic effects were significant, indicating nonlinear effects of these variables. The effects of NaCl and temperature on ThT_{max} are shown in Table 4. Although the effects were nonlinear and significant, the variations in

Table 5. Mean Values of t_{ThTmax} for Particular Parameter Settings That Illustrate Significant 2-Way Interactions in the Factorial Analysis[a]

CaCl$_2$ (mM)	90 °C	110 °C
20	8.49 (2.49)	3.13 (1.04)
60	3.73 (0.97)	2.39 (0.27)
NaCl (mM)	pH 1.5	pH 2.5
25	3.52 (1.02)	7.87 (2.79)
75	2.75 (0.88)	3.59 (0.97)
CaCl$_2$ (mM)	pH 1.5	pH 2.5
20	3.73 (1.20)	7.89 (2.79)
60	2.54 (0.48)	3.57 (0.95)

[a] Each value of t_{ThTmax} is the mean from 4 runs, in which other factors varied. Figures in parentheses are standard errors.

shown in Figure 3, which reveals a strong curvature in the pH effect (consistent with the significant pH*pH effect in Table 2), and shows that the extent of curvature depended on the temperature. Figure 3 was plotted using data from star points and center points, but contour plots constructed using factorial points had a very similar shape, so the pH 3 star point (run 26) did not appear to have undue influence in Figure 3.

NaCl and CaCl$_2$ had a synergistic effect on $(df/dt)_{max}$ as shown by a significant ($p < 0.05$) and moderately strong NaCl*CaCl$_2$ effect in the factorial regression (Table 3). The mean values in Table 6 show that increasing [NaCl] at low [CaCl$_2$] or *vice versa* increased $(df/dt)_{max}$ by approximately 100 FU·h^{-1}. However the effect of increasing both salts simultaneously was to increase $(df/dt)_{max}$ by over 300 FU·h^{-1}.

There were several significant 3-way interactions in the factorial regression, and even the 4-way interaction was significant (Table 3). The 3-way interactions were generally consistent with the 2-way interactions. For example for t_{ThTmax}, NaCl*CaCl$_2$ ($p < 0.05$), NaCl*pH ($p < 0.01$) and CaCl$_2$*pH ($p < 0.05$) contributed to the NaCl*CaCl$_2$*pH interaction ($p < 0.05$).

Transmission Electron Microscopy. Selected TEM images are shown in Figure 4 and Figure 5. Comparing the images from run 1 and run 24 in Figure 4 (panes A and B respectively) shows the effect on fibril morphology of changing the heating temperature from 100 °C (run 1) to 120 °C (run 24) with 50 mM NaCl, 40 mM CaCl$_2$ and pH 2. Run 1 produced a mixture of long semiflexible fibrils and short wormlike fibrils, very similar to the mixture seen at pH 2 and 80 °C with 80−100 mM NaCl or 60 mM CaCl$_2$.[3] Increasing the heating temperature to 120 °C produced fibrils that were straight or gently curved, which suggests increased stiffness. Fibrils from run 24 looked quite similar to those produced by heating at 120 °C at pH 2 in the absence of added salt.[9] The kinetics of fibril formation were also quite different between runs 1 and 24 (Table 1). In run 24, ThT fluorescence increased faster than in run 1, and reached a higher maximum value.

Comparing images from runs 1, 25, and 26 (panes A, C and D in Figure 4) shows the effect of changing pH while heating at 100 °C with 50 mM NaCl and 40 mM CaCl$_2$. At pH 1 (run 25, pane C), fibrils had a curled, twisted appearance, similar to fibrils at pH 2 in run 1 and to those seen at high salt concentration in earlier work at pH 2 and 80 °C.[3] However the long semiflexible fibrils occasionally seen at pH 2 were not seen at pH 1. At pH 3

Table 6. Mean values of $(df/dt)_{max}$ for particular parameter settings that illustrate significant 2-way interactions in the factorial analysis. Each value of $(df/dt)_{max}$ is the mean from 4 runs, in which other factors varied. Figures in brackets are standard errors

temp (°C)	pH 1.5	pH 2.5
90	182.0 (77.28)	132.3 (78.12)
110	339.1 (63.33)	146.6 (64.06)
CaCl$_2$ (mM)	25 mM NaCl	75 mM NaCl
20	69.1 (38.32)	164.1 (77.39)
60	177.2 (49.21)	389.6 (32.50)
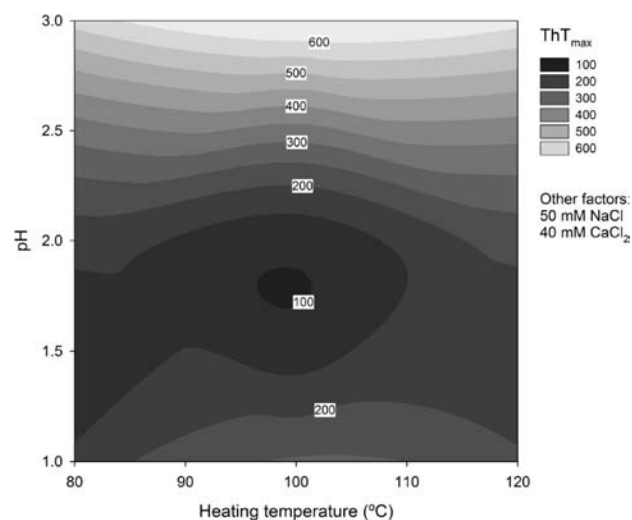
Figure 3. Contour plot showing the interacting effects of heating temperature and pH on ThT$_{max}$. Center points and star points for pH and heating temperature were used to construct the plot, and NaCl and CaCl$_2$ were kept constant at 50 mM and 40 mM respectively.

(run 26, pane D), fibrillar structures were entwined in dense networks, in which individual fibrils could not be clearly distinguished. Fibrils that were not in networks were all <200 nm, and most were 50−100 nm long, with apparently random curvature and nonuniform thickness. The t_{ThTmax} for runs 25 and 26 was less than half that for run 1, and both reached a higher ThT$_{max}$ (Table 1). However ThT$_{max}$ for run 26 was more than twice that for run 25, and $(df/dt)_{max}$ was correspondingly higher.

Comparing images from run 13 and run 17 in Figure 5 (panes A and B respectively) shows the effect of increasing the heating temperature from 90 °C (run 13) to 110 °C (run 17) with 75 mM NaCl and 60 mM CaCl$_2$ at pH 2.5. In both cases fibrils were tightly curled and entangled in localized networks up to ∼1 μm across. As well as being curled, the fibrils appeared to be twisted along their axis, as indicated by periodic variations in their width and brightness. No clear differences between fibrils from run 13 and run 17 could be distinguished, indicating that heating temperature made little difference under these conditions. ThT fluorescence kinetic parameters (Table 1) also showed little difference between these runs.

Figure 5 also shows the difference in fibril morphology between run 19, in which no NaCl was added, and run 20, in which 100 mM
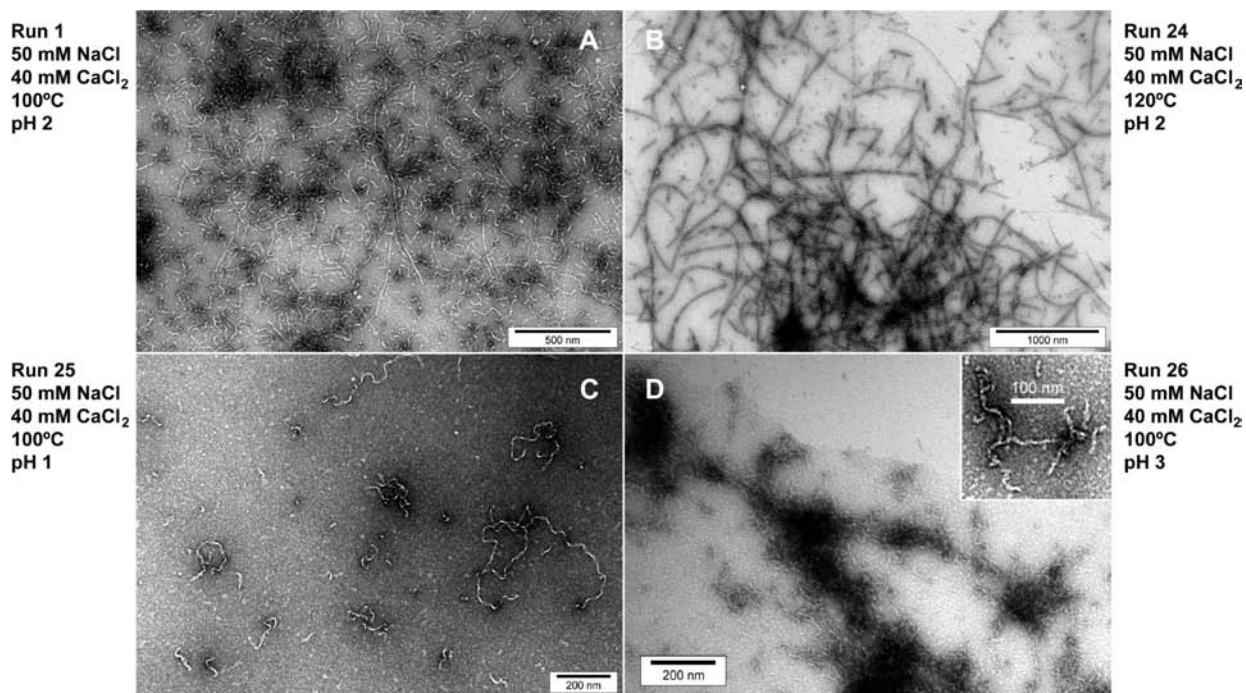
Figure 4. Effect of heating temperature and pH on nanofibril morphology at intermediate salt content. Images are from negative stain TEM of samples heated for 2 h.
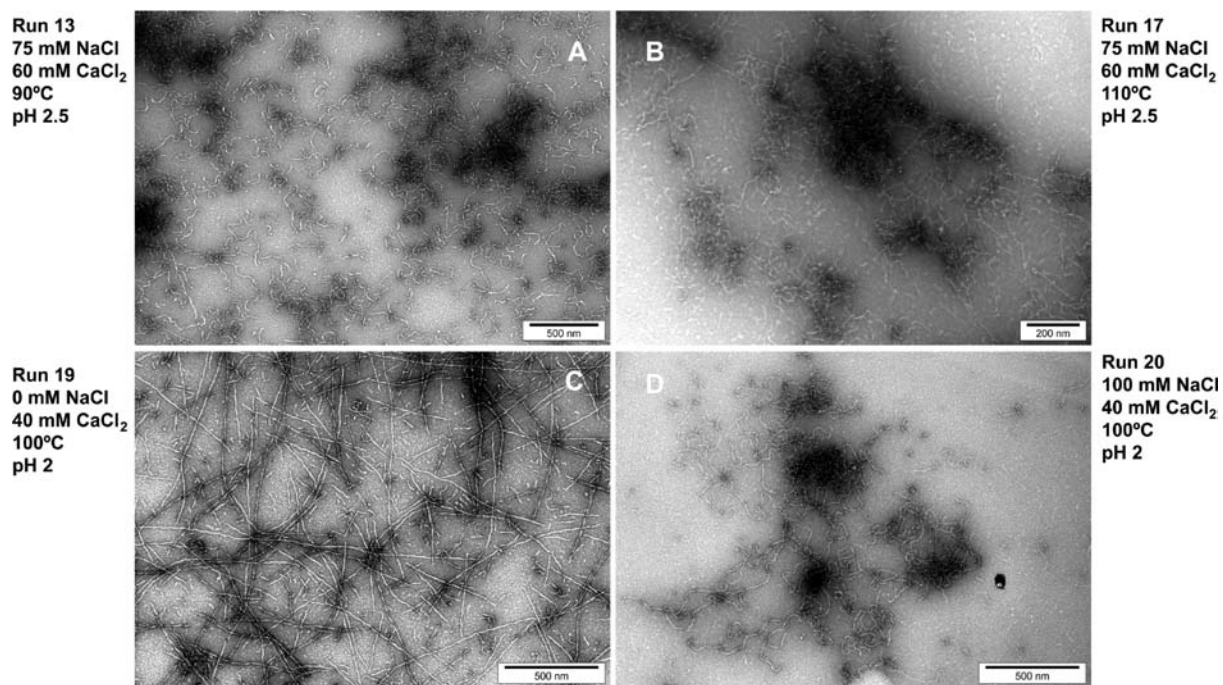

Figure 5. Effect of heating temperature on nanofibril morphology at high salt concentration (A, B) and effect of NaCl on nanofibril morphology at intermediate conditions (C, D). Images are from negative stain TEM of samples heated for 2 h.

NaCl was present (panes C and D respectively). For both runs there was 40 mM CaCl$_2$ present, the heating temperature was 100 °C and the pH was 2.0. The NaCl made a dramatic difference; without added NaCl the fibrils were predominantly long and semiflexible, whereas the fibrils with 100 mM NaCl were tightly

curled and entwined in local networks. The extra NaCl increased the rate of self-assembly (Table 1), but there was little difference in ThT$_{max}$ between the two runs.

The fibrils with 100 mM NaCl (Figure 5 pane D) appeared to be twisted, as commonly seen at high salt concentration,[3] and

with alternating stiff and flexible portions. Fibrils looked like thin, twisted tapes, and it appeared that the portions lying parallel to the plane of view resisted bending in the same plane, whereas those lying perpendicular to the plane were easily bent.

■ DISCUSSION

This study confirms earlier work regarding the individual impact of heating temperature, pH and salt concentration of the kinetics of β-lactoglobulin self-assembly and fibril morphology.[3,9] It also extends previous work to look at more extreme conditions and interactions between these factors.

The most striking feature of the results was the very high ThT fluorescence readings in run 26 (50 mM NaCl, 40 mM CaCl$_2$, 100 °C heating, pH 3.0), and the speed with which they were reached. Conditions in run 26 apparently favored very rapid self-assembly, probably because the high pH (relative to other runs), compounded with charge-shielding effects of salts, meant that electrostatic repulsion between fibril building blocks was minimized. Resulting fibrils were short and irregular, suggesting haphazard, uncontrolled self-assembly. Although these fibrils had high ThT fluorescence, their appearance was quite different from traditional "amyloid-like" fibrils, and their structure may also be different.

Statistically significant interactions between factors influencing protein self-assembly have apparently not been reported before. The significant 2-way interactions may indicate which factors were limiting self-assembly at each condition.

The CaCl$_2$*temperature interaction had a significant and moderately strong effect on kinetic parameters. CaCl$_2$ seemed to be limiting at 90 °C but not at 110 °C. In earlier work we suggested that Ca^{2+} ions may enhance the strength and/or duration of interactions between assembling species via a bridging mechanism involving cation$-\pi$ interactions.[3] Molecular mobility would be higher at 110 °C than at 90 °C, increasing the frequency and force of collisions between assembling species. Cation$-\pi$ interactions may be too weak to influence the movement of faster-moving molecules at 110 °C.

The NaCl*pH and CaCl$_2$*pH interactions were significant for t_{ThTmax} but not for $(df/dt)_{max}$ or ThT$_{max}$. This suggested that the concentration of cations limited the initial stages of self-assembly, before the maximum rate had been attained. Table 5 shows that NaCl and CaCl$_2$ had large effects at pH 2.5, but much smaller effects at pH 1.5, where the hydronium ion activity would be 10-fold greater.

At each pH condition, the mean values of t_{ThTmax} were very similar for 25 mM NaCl vs 20 mM CaCl$_2$ and 75 mM NaCl vs 60 mM CaCl$_2$. This argues against any effect of Cl$^-$ at these concentrations, which is consistent with earlier findings.[3] It also suggests that Na$^+$ and Ca^{2+} had approximately the same ability to promote self-assembly under these conditions. They may have shielded electron-rich or negatively charged regions of self-assembling species, reducing electrostatic repulsion and facilitating self-assembly. (Although most anionic amino acids would be protonated at pH 2.5, a small fraction of aspartic acid and glutamic acid residues would still bear a negative charge. For aspartic acid, the side chain pK_a is 3.71, so the Henderson−Hasselbalch equation predicts 5.8% ionized residues at pH 2.5, and for glutamic acid (side chain pK_a 4.15) the proportion is 2.2%.)

Our earlier work on the kinetics of self-assembly at 80 °C and pH 2 showed that NaCl and CaCl$_2$ had approximately equal effects on $(df/dt)_{max}$, but CaCl$_2$ was much more effective at

shortening the lag phase.[3] The conditions of the present work were somewhat different, particularly in the factorial runs for which the interactions were significant (25−75 mM NaCl, 20−60 mM CaCl$_2$, 90−110 °C, pH 1.5−2.5). This may explain why lag phases were very short or absent in the present work (except for runs 10 and 23), and Na$^+$ and Ca^{2+} had almost equivalent effects on t_{ThTmax}.

Temperature*pH effects on $(df/dt)_{max}$ can be understood by considering the effect of pH on the thermal stability of β-lactoglobulin. At pH 2.5 the thermal transition temperature T_m is 78.8 °C, and it increases to 83.3 °C at pH 1.5.[15] At pH 2.5 the lowest heating temperature used in factorial runs (90 °C) is 11.2 °C above T_m, so denaturation would proceed quickly. However at pH 1.5 the heating temperature is only 6.7 °C above T_m, so the rate of denaturation may be limited by temperature. The added NaCl and CaCl$_2$ in our experiments may have enhanced the stabilizing effects of low pH.[16,17]

Fibril morphologies were largely in keeping with earlier findings, with the exception of run 26, which is discussed above. Fibrils were short and curly when heated at high ionic strength, and morphology changed little when pH was varied between 1 and 2.5, confirming our work with NaCl or CaCl$_2$ alone and in the pH range 1.6−2.4.[3] Heating at 120 °C gave long semiflexible fibrils similar in appearance to others made at 120 °C without added salts.[9]

With the exception of run 26, there did not seem to be a strong link between the kinetics of fibril formation and the morphology of fibrils. For example, runs 1 and 13 (Figure 4 pane A and Figure 5 pane A, respectively) produced morphologically similar fibrils under similar conditions, but at quite different rates.

Similarly, fibrils from runs 19 and 24 were similar in appearance (Figure 5 pane C and Figure 4 pane B respectively), but were formed under somewhat different conditions and at quite different rates.

This work has shown how the rate of β-lactoglobulin self-assembly into nanofibrils and the yield of fibrils (ThT$_{max}$) can be manipulated using synergies between salt content, pH and heating temperature. It has illustrated the range of fibril morphologies that can be created by varying conditions, and shown that a given morphology can be produced several different ways. The range of β-lactoglobulin fibril morphologies seen here lends support to the suggestion by Chiti and Dobson[18] that "each protein sequence can form a spectrum of structurally distinct fibrillar aggregates and that kinetic factors can dictate which of these alternatives is dominant under given circumstances."

It remains to be seen whether there is a link between functionality (e.g., rheological properties) and the kinetics of self-assembly and/or the morphology of β-lactoglobulin nanofibrils.

■ ASSOCIATED CONTENT

Ⓢ **Supporting Information.** Analytical derivation of kinetic parameters. This material is available free of charge via the Internet at http://pubs.acs.org.

■ AUTHOR INFORMATION

Corresponding Author
*E-mail s.loveday@massey.ac.nz. Fax: +64 6 350 5655. Phone: +64 6 356 9099.

■ REFERENCES

(1) Vernaglia, B. A.; Huang, J.; Clark, E. D. Guanidine hydrochloride can induce amyloid fibril formation from hen egg-white lysozyme. *Biomacromolecules* **2004**, *5*, 1362–1370.

(2) Gosal, W. S.; Clark, A. H.; Ross-Murphy, S. B. Fibrillar β-lactoglobulin gels: Part 3. Dynamic mechanical characterization of solvent-induced systems. *Biomacromolecules* **2004**, *5*, 2430–2438.

(3) Loveday, S. M.; Wang, X. L.; Rao, M. A.; Anema, S. G.; Creamer, L. K.; Singh, H. Tuning the properties of β-lactoglobulin nanofibrils with pH, NaCl and CaCl$_2$. *Int. Dairy J.* **2010**, *20*, 571–579.

(4) Yan, H.; Nykanen, A.; Ruokolainen, J.; Farrar, D.; Gough, J. E.; Saiani, A.; Miller, A. F. Thermo-reversible protein fibrillar hydrogels as cell scaffolds. *Faraday Discuss.* **2008**, *139*, 71–84.

(5) Pilkington, S. M.; Roberts, S. J.; Meade, S. J.; Gerrard, J. A. Amyloid fibrils as a nanoscaffold for enzyme immobilization. *Biotechnol. Prog.* **2009**, *26*, 93–100.

(6) Humblet-Hua, K. N. P.; Scheltens, G.; van der Linden, E.; Sagis, L. M. C. Encapsulation systems based on ovalbumin fibrils and high methoxyl pectin. *Food Hydrocolloids* **2010**, *25*, 307–314.

(7) Hill, E. K.; Krebs, B.; Goodall, D. G.; Howlett, G. J.; Dunstan, D. E. Shear flow induces amyloid fibril formation. *Biomacromolecules* **2006**, *7*, 10–13.

(8) Akkermans, C.; van der Goot, A. J.; Venema, P.; van der Linden, E.; Boom, R. M. Formation of fibrillar whey protein aggregates: Influence of heat and shear treatment, and resulting rheology. *Food Hydrocolloids* **2008**, *22*, 1315–1325.

(9) Loveday, S. M.; Wang, X. L.; Rao, M. A.; Anema, S. G.; Singh, H. β-Lactoglobulin nanofibrils: Effect of temperature on fibril formation kinetics, fibril morphology, and the rheological properties of fibril dispersions. *Food Hydrocolloids* **2011**, in press.

(10) Pearce, F. G.; Mackintosh, S. H.; Gerrard, J. A. Formation of amyloid-like fibrils by ovalbumin and related proteins under conditions relevant to food processing. *J. Agric. Food Chem.* **2007**, *55*, 318–322.

(11) Mudgal, P.; Daubert, C. R.; Foegeding, E. A. Cold-set thickening mechanism of β-lactoglobulin at low pH: Concentration effects. *Food Hydrocolloids* **2009**, *23*, 1762–1770.

(12) Kroes-Nijboer, A.; Venema, P.; Bouman, J.; van der Linden, E. The critical aggregation concentration of β-lactoglobulin-based fibril formation. *Food Biophys.* **2009**, *4*, 1–5.

(13) Bolder, S. G.; Vasbinder, A. J.; Sagis, L. M. C.; van der Linden, E. Heat-induced whey protein isolate fibrils: Conversion, hydrolysis, and disulphide bond formation. *Int. Dairy J.* **2007**, *17*, 846–853.

(14) Montgomery, D. C.; Runger, G. C.; Hubele, N. F. *Engineering statistics*, 3rd ed.; John Wiley and Sons, Inc.: New York, 2004.

(15) Kella, N. K.; Kinsella, J. E. Enhanced thermodynamic stability of β-lactoglobulin at low pH. A possible mechanism. *Biochem. J.* **1988**, *255*, 113–118.

(16) Boye, J. I.; Alli, I.; Ramaswamy, H.; Raghavan, V. G. S. Interactive effects of factors affecting gelation of whey proteins. *J. Food Sci.* **1997**, *62*, 57–65.

(17) Harwalkar, V. R.; Kalab, M. Thermal denaturation and aggregation of β-lactoglobulin at pH 2.5 - effect of ionic-strength and protein-concentration. *Milchwissenschaft* **1985**, *40*, 31–34.

(18) Chiti, F.; Dobson, C. M. Protein misfolding, functional amyloid, and human disease. *Annu. Rev. Biochem.* **2006**, *75*, 333–366.

8474

dx.doi.org/10.1021/jf201870z |*J. Agric. Food Chem.* 2011, 59, 8467–8474